Published in final edited form as:
Sci Transl Med. 2016 May 25; 8(340): 340ra74. doi:10.1126/scitranslmed.aac4296.

Up-regulation of miR-31 in human atrial fibrillation begets the arrhythmia by depleting dystrophin and neuronal nitric oxide synthase

Svetlana N. Reilly[#1,†], **Xing Liu**[#1], **Ricardo Carnicer**[1], **Alice Recalde**[1], **Anna Muszkiewicz**[2], **Raja Jayaram**[1], **Maria Cristina Carena**[1], **Rohan Wijesurendra**[1], **Matilde Stefanini**[1], **Nicoletta C. Surdo**[1], **Oliver Lomas**[1], **Chandana Ratnatunga**[3], **Rana Sayeed**[3], **George Krasopoulos**[3], **Timothy Rajakumar**[4], **Alfonso Bueno-Orovio**[2], **Sander Verheule**[5], **Tudor A. Fulga**[4], **Blanca Rodriguez**[2], **Ulrich Schotten**[5], and **Barbara Casadei**[#1,†]

[1]Division of Cardiovascular Medicine, Radcliffe Department of Medicine, University of Oxford, John Radcliffe Hospital, Oxford OX3 9DU, UK [2]Department of Computer Science, University of Oxford, Oxford OX1 3QD, UK [3]Cardiothoracic Surgery, Oxford Heart Centre, John Radcliffe Hospital, Oxford OX3 9DU, UK [4]Weatherall Institute of Molecular Medicine, Radcliffe Department of Medicine, University of Oxford, Oxford OX3 9DS, UK [5]Department of Physiology, University of Maastricht, 6211 LK Maastricht, Netherlands

[#] These authors contributed equally to this work.

Abstract

Atrial fibrillation (AF) is a growing public health burden, and its treatment remains a challenge. AF leads to electrical remodeling of the atria, which in turn promotes AF maintenance and resistance to treatment. Although remodeling has long been a therapeutic target in AF, its causes remain poorly understood. We show that atrial-specific up-regulation of microRNA-31 (miR-31) in goat and human AF depletes neuronal nitric oxide synthase (nNOS) by accelerating mRNA decay and alters nNOS subcellular localization by repressing dystrophin translation. By shortening action potential duration and abolishing rate-dependent adaptation of the action potential duration, miR-31 overexpression and/or disruption of nNOS signaling recapitulates features of AF-induced remodeling and significantly increases AF inducibility in mice in vivo. By contrast, silencing miR-31 in atrial myocytes from patients with AF restores dystrophin and nNOS and normalizes action potential duration and its rate dependency. These findings identify atrial-specific up-regulation of miR-31 in human AF as a key mechanism causing atrial dystrophin and nNOS

[†]Corresponding author. barbara.casadei@cardiov.ox.ac.uk (B.C.); svetlana.reilly@cardiov.ox.ac.uk (S.N.R.).

Author contributions: B.C. and S.N.R. conceived the study, designed the experiments, and wrote the manuscript. S.N.R. and X.L. carried out and analyzed most of the experimental work, with the exception of the in vivo experiments in mice (performed by R.C. and A.R.). A.M., A.B.-O., and B.R. carried out the in silico simulation. U.S. and S.V. provided tissue samples from the goat model and supervised the in vivo experiments in mice. R.W., O.L., R.J., C.R., R.S., G.K., N.C.S., M.C.C., and M.S. were involved in consenting patients, collecting and processing human atrial tissue samples, and isolating and culturing human atrial myocytes. T.A.F. and T.R. designed the miR-31 reporter assays. All authors discussed the results and had the opportunity to comment on the manuscript.

Competing interests: B.C. and S.N.R. hold a UK patent related to this work, with application no. 14/895468.

Data and materials availability: All data and materials are available and shown.

Europe PMC Funders Author Manuscripts

depletion, which in turn contributes to the atrial phenotype begetting this arrhythmia. miR-31 may therefore represent a potential therapeutic target in AF.

Introduction

Atrial fibrillation (AF) is the most common heart rhythm disorder worldwide and a major public health burden due to its impact on the risk of stroke and heart failure (1). The last 20 years have witnessed a significant increase in the incidence of AF in the developed and developing world, caused by population aging and the rising prevalence of risk factors for AF, such as hypertension, obesity, and diabetes (2). To date, pharmacological strategies to restore sinus rhythm (SR) in patients with AF have targeted ion channels. This approach has been marred by poor efficacy, lack of benefit on patient outcomes, and safety concerns related to their propensity to induce life-threatening ventricular arrhythmias (3, 4). Similarly, whether AF ablation techniques are effective in restoring SR in the long term or in improving survival and the risk of stroke remains to be demonstrated (1). Underlying AF resistance to treatment is the ability of the arrhythmia to sustain itself by inducing electrical and structural remodeling of the atria, which in turn promotes AF maintenance and increases vulnerability to relapse (5). The mechanisms leading to atrial remodeling in AF are poorly understood, and identification of atrial-specific molecular targets upstream of this process has been the focus of intense investigation.

Nitric oxide (NO) is known to regulate atrial electrical properties (6) and exert antifibrotic and antithrombotic actions (7). Short-term AF has been reported to induce a profound reduction in atrial NO release in animal models and inconsistent changes in the “endothelial” isoform of NO synthase (eNOS) (7, 8). A “neuronal” NOS isoform (nNOS) is also constitutively expressed in the sarcoplasmic reticulum and sarcolemmal membrane of cardiomyocytes [as part of the dystrophin-associated glycoprotein complex (9)] where nNOS-derived NO regulates sarcolemmal ion conductance (6, 10) and calcium fluxes under basal conditions and in response to mechanical stress (11) and prevents arrhythmic death in mice after myocardial infarction (10). Basal blood flow in the human coronary vascular bed and perfusion of the exercising muscle are also regulated by nNOS-derived NO (12, 13). Loss of sarcolemmal nNOS in the skeletal muscle of patients with Duchenne muscular dystrophy (DMD) (14) leads the dystrophin-deficient muscle to ischemia during contraction (15). Thus, subcellular localization of nNOS signaling may be an important function of the dystrophin-associated glycoprotein complex.

Here, we show that atrial-specific up-regulation of microRNA-31 (miR-31) in goats and in patients with AF leads to nNOS depletion (by accelerating nNOS mRNA decay) and disrupts nNOS sarcolemmal localization by translational repression of dystrophin, resulting in loss of sarcolemmal nNOS and a profound reduction in NOS activity. By shortening action potential duration (APD) and abolishing APD rate-dependent adaptation, miR-31 up-regulation and disruption of nNOS signaling contribute to the AF-induced electrical remodeling of the atrial myocardium and significantly increase AF inducibility in vivo in mice. These data have uncovered similarities between AF-induced molecular and electrical

Europe PMC Funders Author Manuscripts

remodeling of the atrial myocardium and the cardiomyopathy of DMD, and identified miR-31 as a potential therapeutic target for both conditions (16).

Results

AF-induced depletion of nNOS in atrial myocytes contributes to the electrical phenotype that begets AF

We carried out investigations in samples of atrial tissue from patients in SR ($n = 165$) or persistent AF ($n = 51$) (table S1) and from goats after 2 weeks ($n = 11$) or 6 months ($n = 9$) of pacing-induced AF (versus 16 controls in SR). A profound reduction in atrial nNOS protein content and activity (measured as conversion of L-arginine into L-citrulline) in goat atria occurred early (2 weeks) after AF induction and persisted at 6 months (Fig. 1, A and B). Similarly, NOS activity was significantly reduced in human right atrial tissue from patients with persistent AF (Fig. 1C and fig. S1A), where we also identified atrial myocytes as the main source of nNOS depletion (Fig. 1D). Other NOS isoforms did not change significantly in the presence of AF in human or goat atrial tissue (fig. S1).

nNos gene deletion or inhibition with *S*-methylthiocitrulline (SMTC; 100 nM) did not affect the resting membrane potential or the action potential amplitude in murine and human atrial myocytes (table S2). Removing or blocking nNOS significantly reduced APD at 50 and 90% of repolarization (APD_{50} and APD_{90}) (Fig. 1E) and abolished the APD rate-dependent adaptation in atrial myocytes from patients in SR (Fig. 1F), but had no effect in the presence of AF. A shorter APD was also observed in atrial myocytes from $nNos^{-/-}$ mice, in wild-type myocytes upon nNOS inhibition with SMTC (Fig. 1G), and in human atrial myocytes after *nNOS* knockdown by small interfering RNA (fig. S2, A to C).

NO has been shown to regulate several sarcolemmal ion currents by either cyclic GMP (guanosine 5′-monophosphate–mediated) changes in phosphorylation or S-nitrosation of the channel protein (6). In right atrial myocytes from patients in SR, nNOS inhibition resulted in a significant increase in the atrial-specific ultrarapid delayed rectifier K^+ current (I_{Kur}) (Fig. 2, A and B), the transient outward potassium current (I_{to}) (fig. S2D), and the inward rectifier K^+ current (I_{K1}) (Fig. 2C), with a trend toward an increase in the L-type calcium current (I_{CaL}) (fig. S2E). The relative impact of these changes in ion current density on APD_{50} and APD_{90} was evaluated in silico using an experimentally calibrated population of 640 human atrial cell models, sharing the same equations but with differences in ionic conductance and permeability (17). As shown in Fig. 2 (D and E), mimicking the increase of I_{Kur} induced by SMTC reproduced most of the reduction in APD_{50} observed experimentally. Modeling the increase of both I_{Kur} and I_{K1} also recovered the reduction in APD_{90}, whereas the observed changes in I_{to} and I_{CaL} had no impact on APD. Inhibition of I_{Kur} using 4-AP (50 μM) abolished the effect of SMTC on APD in atrial myocytes from patients in SR (fig. S2F).

Together, these findings mimic hallmark features of AF-induced electrical remodeling, which, by facilitating functional reentry, promote induction and maintenance of AF (5). To assess whether loss of nNOS increases AF induction in vivo, we performed atrial burst pacing in $nNos^{-/-}$ mice and their wild-type littermates. AF induction and duration were

significantly higher in *nNos*$^{-/-}$ mice, in the absence of electrophysiological (table S3) or structural cardiac abnormalities (Fig. 2F) (10).

We next investigated the mechanism responsible for nNOS depletion in the fibrillating human atrial myocardium. In skeletal muscle, nNOS is bound to the dystrophin-associated glycoprotein complex, the disruption of which leads to the near disappearance of nNOS at the sarcolemmal membrane, as observed in DMD (14). Dystrophin and nNOS coimmunoprecipitated and colocalized to the sarcolemma of human atrial myocytes in SR, but not in AF (Fig. 3, A to D). In AF, dystrophin—evaluated using antibodies directed to the protein rod domain or the C terminus—and its associated proteins, caveolin-3 and α1-syntrophin, were significantly reduced (Fig. 3,B and E, and fig. S3A). Dystrophin and α1-syntrophin were similarly decreased in atrial tissue from goats after 2 weeks and 6 months of pacing-induced AF (fig. S3, B and C). By contrast, *nNos* gene deletion did not alter atrial dystrophin content in mice (fig. S3D). These findings indicate that reduced availability of nNOS-derived NO in AF contributes to the atrial electrical remodeling induced by the arrhythmia and is sufficient to increase AF induction in vivo.

Atrial-specific miR-31 up-regulation in persistent AF underlies dystrophin and nNOS depletion

As reported in the skeletal muscle of patients with DMD (18), we observed a significant reduction in *nNOS* mRNA in atrial myocytes from patients with AF (Fig. 3F), whereas dystrophin mRNA was unchanged (Fig. 3G). To evaluate whether posttranscriptional regulation of atrial nNOS and dystrophin contributed to their depletion in human AF, we carried out an in silico analysis to identify miRs predicted to target both transcripts in humans. Among these, miR-31 had previously been reported to repress dystrophin translation in the skeletal muscle of patients with DMD (16). In the presence of AF, miR-31 expression was significantly higher in human atrial myocytes and in goat left atrial tissue, but not in goat left ventricular tissue (Fig. 3, H and I).

By contrast, in patients with paroxysmal AF or in those who developed AF after cardiac surgery (tables S4 and S5), atrial miR-31 was not up-regulated (Fig. 4, A and E), and nNOS and dystrophin (expression and protein content) did not differ compared with matched patients in SR (Fig. 4, B to D) or who remained in SR after cardiac surgery (Fig. 4, F to H). These data are in line with evidence indicating that atrial electrical remodeling is not present in patients with paroxysmal AF nor does it precede the occurrence of AF (19, 20).

Prediction algorithms identified one conserved putative miR-31 binding site on the human dystrophin 3′ untranslated region (3′UTR) and five in the human *nNOS* 3′UTR (table S6). Only one of five predicted miR-31 binding sites on *nNOS* 3′UTR (site 5) was shown to be functional in a reporter assay in human kidney cells [human embryonic kidney (HEK) 293T], which also confirmed functionality of the miR-31 binding site in the dystrophin 3′UTR (fig. S4, A to D) (16).

mRNA regulation by small, noncoding miRs is accomplished through the RNA-induced silencing complex (RISC), where Argonaute (Ago) proteins associated with miRs bind to the 3′UTR of mRNAs facilitating their degradation or inhibiting translation (21). In atrial

myocytes from patients with AF, immunoprecipitation of Ago2 (fig. S5A) confirmed the presence of *nNOS* and dystrophin mRNA within the RISC (Fig. 5, A and B). Blocking the corresponding miR-31 binding site with a selective locked nucleic acid (LNA)–enhanced target site blocker (TSB; table S7) reduced the RISC incorporation of the respective mRNA (Fig. 5, A and B) but not of miR-31 (fig. S5B).

To investigate the mode by which miR-31 regulates dystrophin and *nNOS* gene expression, we assessed corresponding mRNA stability in the presence of an miR-31 mimic in human SR myocytes treated with the transcription inhibitor actinomycin D. Under these conditions, miR-31 accelerated the decay of *nNOS* mRNA but not of dystrophin (Fig. 5C and fig. S5, C and D). In agreement with these findings, preventing the binding of miR-31 to nNOS mRNA in AF myocytes using a selective TSB increased *nNOS* mRNA and partially recovered nNOS protein without affecting dystrophin mRNA and protein content (Fig. 5, D and E). By contrast, preventing binding of miR-31 to dystrophin mRNA did not change *nNOS* or dystrophin mRNA but restored dystrophin protein content and partially recovered nNOS (Fig. 5, F and G), indicating that dystrophin affects nNOS protein stability as well as its subcellular localization. Together, these data confirm that miR-31 binds to the 3′UTR of both dystrophin and *nNOS* mRNA in human atrial myocytes, where it leads to a reduction of the respective protein by accelerating *nNOS* mRNA decay and inhibiting the translation of dystrophin mRNA.

Up-regulation of miR-31 affects the electrical phenotype of human atrial myocytes

Antiarrhythmic drugs targeting ion channels may recover SR in patients with AF by suppressing excitability and prolonging the atrial effective refractory period (for example, by lengthening APD). However, because ion channel expression is similar in the atrial and ventricular myocardium, the use of antiarrhythmic agents in patients with AF increases the risk of ventricular arrhythmias (3). Up-regulation of miR-31 in human AF is limited to the atrial myocardium, suggesting that cardiac miR-31 inhibition may be a safer “upstream” approach for reversing or preventing AF-induced electrical remodeling and promoting the maintenance of SR. miR-31 inhibition increased dystrophin and nNOS protein content in atrial myocytes from patients with AF (Fig. 6, A and B, and fig. S4B) and also restored APD and APD rate-dependent adaptation (Fig. 6, C and D); both effects were reversed by pharmacological nNOS inhibition, confirming that the effects of miR-31 on the electrical phenotype of human atrial myocytes are mediated by nNOS-derived NO.

miR-31 inhibition had no measurable effect on miR-31 expression, dystrophin, or nNOS in atrial myocytes from patients in SR (Fig. 6, E to G); however, in these cells, increasing intracellular miR-31 expression (by using a miR-31 mimic) reduced *nNOS* mRNA and the protein content of dystrophin and nNOS and shortened APD (Fig. 7, A to E). In summary, by accelerating *nNOS* mRNA decay and repressing dystrophin translation, up-regulation of miR-31 in the atrial myocardium of patients with AF results in a profound reduction in NO signaling, which in turn leads to an atrial electrical phenotype that sustains AF (Fig. 7F).

Discussion

An important advance in our understanding of AF has been the recognition that by remodeling atrial electrical and structural properties, AF promotes its maintenance and resistance to treatment (5). Changes in the expression of genes encoding sarcolemmal ion channels contribute to AF-induced atrial remodeling, and miRs have previously been reported to target the expression of ion channels subunits involved in this process (22). Here, we have identified myocardial *nNOS* depletion as a novel molecular mechanism upstream of the atrial electrical substrate that sustains AF in humans.

Our findings draw interesting parallels between AF and DMD. By reducing S-nitrosation (and increasing activity) of class II histone deacetylase, nNOS depletion plays an important role in the epigenetic regulation of gene expression in DMD, contributing to muscle redox imbalance and injury (23). Increased oxidative stress is a common feature of the dystrophic heart muscle (24), the fibrillating human atrial myocardium (25), and the myocardium of mice lacking nNOS (26). nNOS depletion or inhibition has been linked to impaired muscle perfusion (12, 15), reduced dystrophin to altered Ca^{2+} homeostasis, increased membrane fragility, and cell death (24), suggesting that atrial nNOS/dystrophin depletion secondary to miR-31 up-regulation may affect all aspects of AF-induced atrial remodeling. The effects of miR-31 up-regulation on the atrial electrical phenotype were dependent on nNOS-derived NO and were reproduced in atrial myocytes from the *nNos*$^{-/-}$ mouse in which dystrophin content was unaltered, suggesting that the observed reduction in dystrophin in human AF had no direct impact on atrial action potential characteristics.

miR-31 inhibition in atrial myocytes from patients with AF resulted in a significant prolongation of APD that was reversed upon nNOS inhibition, whereas the use of a mimic to induce miR-31 overexpression in SR myocytes produced comparatively smaller effects. To what extent the transfected miR-31 was bio-active is unclear; nevertheless, dystrophin and nNOS content decreased in response to the miR-31 mimic, and the APD shortening was similar to that observed after nNOS inhibition in SR atrial myocytes, suggesting that remodeling of NO-sensitive targets by AF may account for the apparently larger effect of miR-31 inhibition on APD in AF myocytes.

We did not investigate whether miR-31 also has a role in the down-regulation of ion channels subunits in human AF. However, APD shortening and the increase in repolarizing K^+ currents were detected after acute nNOS inhibition in atrial myocytes from patients in SR and from wild-type mice as well as in AF myocytes after incubation with an miR-31 blocker, indicating that constitutive myocardial NO production can rapidly modulate sarcolemmal ion currents, as suggested by previous investigations using NO donors (6). NO donors, however, do not consistently reproduce the effects of NO released by constitutive NOS isoforms (27, 28), because NOS subcellular localization is a critical determinant of myocardial NO signaling (10, 11). nNOS inhibition did not mimic all the changes in atrial ion currents described in long-standing persistent AF, where I_{CaL} and I_{to} are substantially decreased, I_{Kur} is reduced or unchanged, and I_{K1} is increased (29). However, in silico modeling indicated that the increase in I_{Kur} and I_{K1} accounted for most of the effect of

nNOS inhibition on APD_{50} and APD_{90} in human atrial myocytes, whereas the impact of the relatively small changes in I_{CaL} and I_{to} on APD was negligible.

Our findings indicate that depleted atrial nNOS in the early stages of AF helps to stabilize arrhythmia by shortening atrial refractoriness before changes in ion channel expression. Because up-regulation of miR-31 is atrial-specific and its effects on atrial electrical properties are rapidly reversible, interventions targeted to this pathway may provide an effective and safer therapeutic option for patients with AF. In particular, because the efficacy of AF ablation procedures in the medium to long term is relatively weak and repeated interventions are often required to restore SR in symptomatic patients with persistent AF (30), adjuvant interventions, such as local inhibition of relevant miRs, may prove an effective strategy for reversing the atrial substrate that sustain AF and reducing the need for reintervention. More advanced delivery strategies (for example, tissue-specific vectors and promoters), as well as the identification of mechanisms leading to atrial miR-31 up-regulation by AF, may circumvent the lack of cell-specific targeting that is currently a major drawback of miR manipulation for therapeutic purposes (31).

Materials and Methods

Study design

The primary aims of this study were to evaluate whether NOS activity and constitutive NOS isoforms were reduced in the presence of AF and to investigate the cause and impact of impaired atrial NO production on AF-induced electrical remodeling in humans. We estimated that to have >80% power at $P = 0.05$ to detect a proportional reduction in NOS activity of 30% in AF versus SR, we would need ≥15 patients per group. The same sample size would allow us to detect 25% differences in protein density of NOS isoforms between AF and SR with >90% statistical power. The explorative phase of the study was conducted using whole-tissue homogenates from samples of the right atrial appendage obtained from patients older than 18 years undergoing first-time elective cardiac surgery. Findings were subsequently validated in human right atrial myocytes. Time- and chamber-specific trends in the reduction of nNOS activity/protein were explored in a goat model of pacing-induced AF. Follow-up mechanistic studies were performed in isolated human atrial myocytes, in goat atrial and ventricular tissues, and in *nNos*$^{-/-}$ mice and their wild-type littermates.

For ion current measurements, we used three to six atrial myocytes per patient/mice and planned the sample size, taking into consideration the variability of the measurements in our hands and the effect size reported by other investigators in experiments using NO donors or NOS inhibition in cardiomyocytes (6). Inhibitors and mimics were used to assess both the loss and gain of function of miR-31 on dystrophin and nNOS mRNA and protein content and on APD and APD rate-dependent adaptation in human atrial myocytes. In vivo studies were not randomized, but experiments were carried out and analyzed with the operator blind of the genotype. Similarly, analysis of current traces and all other experimental data was carried out in a blinded fashion. No data were excluded from analysis, except those obtained in atrial myocytes that did not survive the whole duration of the APD rate-dependent adaptation protocol (24 of 209 myocytes).

Investigations were approved by the local Research Ethics Committees or performed according to the European directive on laboratory animals (86/609/EEC) or the Home Office Guidance on the Operation of Animals (Scientific Procedures) Act 1986. All patients gave informed written consent. A total of 278 patients, 77 mice, and 36 goats were included in the study.

Animals

Female goats (45 to 61 kg) were instrumented, as described previously (32). AF was induced by repetitive burst pacing and maintained for 2 weeks ($n = 11$) or 6 months ($n = 9$); sham-operated goats in SR ($n = 16$) were used as controls. Homozygous *nNos*$^{-/-}$ mice of both sexes (3 to 4 months old, $n = 37$) were compared to their wild-type littermates ($n = 40$).

NOS activity in human and goat atrial homogenates

Atrial NOS activity was evaluated by conversion of [^{14}C]L-arginine (Amersham) to citrulline (in the presence of the arginase inhibitor *N*ω-hydroxy-nor-arginine; Calbiochem) by high-performance liquid chromatography (25). Values are expressed as *N*ω-nitro-L-arginine methyl ester hydrochloride (L-NAME)–inhibitable fraction.

Western blots

Immunoblotting in human, goat, and murine atrial homogenates and in human atrial myocytes was performed as described previously (25). We used primary antibodies raised against nNOS (Santa Cruz Biotechnology), eNOS (BD Transduction Laboratories), dystrophin [NCL-DYS1 (rod domain) and NCL-DYS2 (C terminus); Novocastra, Leica Biosystems, or Thermo Fisher Scientific], caveolin-3 and iNOS (inducible isoform of NOS) (Abcam), α1-syntrophin (AbD Serotec), α-actinin, and GAPDH (Millipore). Immunodetection of the primary antibodies was performed using horseradish peroxidase–conjugated secondary antibodies (Promega). For some experiments, membrane and cytosolic fractions were separated by multiple centrifugation steps, as described previously (33).

Immunoprecipitation assay for dystrophin and nNOS in right atrial homogenates

Atrial samples were homogenized on ice, centrifuged (13,000*g* at 4°C for 15 min), and immunoabsorbed with anti-nNOS or anti-dystrophin antibodies (NCL-DYS1). Immune complexes were precipitated for 3 hours by the addition of Protein A/G–conjugated agarose (Santa Cruz) and immunoblotted with anti-nNOS and anti-dystrophin antibodies; agarose beads with immunoglobulin (Ig) G/A alone were used as control for nonspecific binding.

Immunohistochemistry

Immunostaining was performed in OCT (optimal cutting temperature compound)–embedded cryosections of human atrial tissue, whereas colocalization between dystrophin and nNOS was evaluated in human atrial myocytes. Briefly, cryosections or myocytes were fixed in precooled (−20°C) acetone/methanol (1:1) solution, air-dried and rinsed in phosphate-buffered saline (PBS), blocked with serum-free blocking reagent (DAKO, Agilent Technologies), and incubated with an anti-dystrophin or anti-nNOS antibody overnight at 4°C. After multiple rinsing steps with 0.1% PBST (PBS with Tween 20), secondary Alexa

Fluor antibodies (Invitrogen) were applied for 1 hour at room temperature. Imaging was performed using a Zeiss LSM 510 or Leica DM 6000 CFS confocal imaging system.

Quantitative real-time polymerase chain reaction analysis

We compared the expression of dystrophin, nNOS, and miR-31 transcripts using quantitative polymerase chain reaction (qPCR) in human and goat cardiac tissue or in human atrial myocytes. Briefly, total RNA was extracted with the miRNeasy Kit (QIAGEN) or mirVana Kit (Applied Biosystems) according to the manufacturer's instruction. Quantitative reverse-transcriptase PCR (qRT-PCR) was carried out using the QuantiTect Reverse Transcription Kit (QIAGEN) and TaqMan Gene Expression Assays for dystrophin and nNOS (Applied Biosystems; assay IDs: human dystrophin 3′UTR, Hs01049460_m1; human dystrophin central domain, Hs00758098_m1; human dystrophin 5′UTR, Hs01049418_m1; and human nNOS, Hs00167223_m1). For miR-31 qRT-PCR, the TaqMan MicroRNA Reverse Transcription Kit, TaqMan MicroRNA Assay stem-loop primers, and TaqMan Universal Master Mix were used (all from Applied Biosystems).

For the gene expression assay on transfected human myocytes, a preamplification step was used before the qPCR, in accordance with the manufacturer's instruction. Each reaction was performed in duplicates using ABI 7900HT Detection System (Applied Biosystems). Relative quantification was obtained by using the comparative threshold cycle method ($2^{-\Delta\Delta Ct}$); the expression of the target gene was normalized to *GAPDH* or β-*actin* (for dystrophin and nNOS transcripts), or to *snoU6* (for miR-31expression) and related to a control reference sample.

Ribonucleoprotein immunoprecipitation with Ago2 in human right atrial myocytes

The ribonucleoprotein immunoprecipitation (RIP) assay was carried out to assess interaction between dystrophin or *nNOS* mRNA with miR-31 within the RISC. Human atrial myocytes from patients with AF were transfected for 48 hours with an LNA-based miR-31 TSB (20 nM) for dystrophin or *nNOS*, or the corresponding nontargeting negative control. RIP was performed using the Magna RIP kit (Millipore). Briefly, cells were washed in PBS (three times) before lysis in 100 μl of complete RIP lysis buffer and incubated with magnetic beads conjugated with anti-Ago2/eIF2C2 antibody (Abcam) or rabbit IgG (Millipore) and rotated overnight at 4°C. Coimmunoprecipitated RNA, including miR/mRNA complexes, was subjected to qPCR and miR qPCR. Expression of dystrophin and *nNOS* genes was normalized to miR-31 and calculated using the comparative threshold cycle method ($2^{-\Delta\Delta Ct}$).

miR-31 target predictions

Using six prediction algorithms, that is, DIANAmT, miRanda, miR-Walk, PicTar5, PITA, and Targetscan (for reference, refer to MiRWalk program: www.umm.uni-heidelberg.de/apps/zmf/mirwalk/serverfull.php), in silico analysis predicted binding of miR-31-5p to nNOS 3′UTR at five sites (table S6).

Reporter assay

All reporter constructs were derived from pcDNA3.1/Hygro(+) vector (Life Technologies). A dual fluorescence reporter (pCMV-dEGFP-SV40-ECFP) was generated by cloning the

dEGFP gene into Bam HI and Not I sites downstream of the cytomegalovirus (CMV) promoter and by replacing the hygromycin resistance gene downstream of the SV40 promoter with enhanced cyan fluorescent protein (ECFP) using sequence overlap extension PCR. A fragment of the dystrophin 3′UTR [~500 base pairs (bp)] or two fragments (named part 1 and part 2, ~500 bp each) of the *nNOS* 3′UTR, centered on each of the predicted miR-31 target binding sites, were cloned into the pCMV-dEGFP-SV40-ECFP vector. Site-directed mutagenesis was used to create reporter constructs in which miR-31 target sites were individually or globally disrupted (fig. S4). HEK293T cells were cotransfected with reporter constructs (250 ng) and miRIDIAN miR-31 mimic (a double-stranded sequence of RNA oligonucleotides) or negative control #1 (10 nM for nNOS sensor and 50 nM for dystrophin sensor, both from Dharmacon) using a polyethylenimine transfection reagent (Invitrogen) in antibiotic-free Dulbecco's modified Eagle's medium containing 2% fetal bovine serum. The effect of miR-31 on GFP (green fluorescent protein) fluorescence was measured by fluorescence-activated cell sorting (FACS) (CyAn, DakoCytomation) 48 hours after transfection. dEGFP (destabilized enhanced GFP) was measured using a 488-nm laser and a 530/40-nm emission filter. ECFP was measured using a 405-nm laser and a 450/50-nm emission filter; ~50,000 (for nNOS sensors) and ~20,000 (for the dystrophin sensors) events were recorded per sample.

Electrophysiological recordings

Whole-cell voltage and current-clamp experiments were carried out in human and murine right atrial myocytes as described in the Supplementary Methods.

In vivo transesophageal burst pacing

AF induction was assessed in isofluorane (2%)–anaesthetized mice by transesophageal burst pacing, as described previously (34). Briefly, a 1.7-French catheter was advanced into the esophagus to capture the atria and deliver the electrical stimuli. Two pairs of intradermal electrodes were implanted to monitor ECG signals throughout the experiment. All electrical signals were preamplified and recorded using the Spike2 software (version 7.09). Each burst was composed of 40 external stimulations at 1.5 times the threshold for atrial capture, starting from a cycle length of 60 ms and decreasing at each successive burst by 2 ms, down to a final cycle length of 10 ms. A series of 25 bursts were repeated three times in each animal. An AF episode was defined as a period of rapid irregular atrial rhythm lasting at least 2 s.

In silico modeling

Simulation studies were conducted using a population of virtual human atrial models based on Maleckar *et al.*'s model (35), as described in the Supplementary Methods.

Statistical analysis

Student's *t* test was used in two-group comparisons. Multiple groups of normally distributed data of similar variance were compared by one- or two-way ANOVA, in some cases, after log transformation. For multiple comparisons, the Bonferroni's corrected *P* value is shown. Kruskal-Wallis test, Mann-Whitney *U* test, or Wilcoxon test was used when the normality

assumption was not met. Categorical variables were compared by χ^2 test; Fisher exact test was used to compare surgical procedures. All statistical analyses were performed using GraphPad Prism v5 or v6.04. A value of $P < 0.05$ was considered statistically significant.

Supplementary Material

Refer to Web version on PubMed Central for supplementary material.

Acknowledgments

We thank A. Jefferson and J. Digby for their assistance in conducting immunofluorescence experiments and K. Clark for his help with FACS experiments and analysis.

Funding: This study was funded by the British Heart Foundation (BHF) Programme Grant (RG/11/15/29375) (to B.C.), the Oxford BHF Centre of Excellence (RE/13/1/3018) (to S.N.R. and R.W.) and, in part, by the Fondation Leducq Network of Excellence (08CVD01) (to B.C., S.N.R., and M.S.), the European Union 7th Framework Programme under Grant Agreement n°261057 [EUTRAF (European Network for Translational Research in Atrial Fibrillation)] (to B.C. and R.C.), an FP7 Marie Curie (Initial Training Network) grant [RADOX (Radical reduction of oxidative stress in cardiovascular disease)] to M.C.C., and a Wellcome Trust studentship to O.L. (099898/Z/12/Z). T.A.F. and T.R. are funded by a Weatherall Institute of Molecular Medicine strategic award and the UK Medical Research Council (#G0902418). B.R. is supported by a Wellcome Trust Senior Research Fellowship (100246/Z/12/Z). A.M. holds an EPSRC (Engineering and Physical Sciences Research Council) scholarship from the Systems Biology Doctoral Training Centre of the University of Oxford.

References and Notes

1. January CT, Wann LS, Alpert JS, Calkins H, Cigarroa JE, Cleveland JC Jr, Conti JB, Ellinor PT, Ezekowitz MD, Field ME, Murray KT, et al. American College of Cardiology/American Heart Association Task Force on Practice Guidelines, 2014 AHA/ACC/HRS guideline for the management of patients with atrial fibrillation: A report of the American College of Cardiology/American Heart Association Task Force on Practice Guidelines and the Heart Rhythm Society. J Am Coll Cardiol. 2014; 64:e1–e76. [PubMed: 24685669]
2. Chugh SS, Havmoeller R, Narayanan K, Singh D, Rienstra M, Benjamin EJ, Gillum RF, Kim Y-H, McAnulty JH Jr, Zheng Z-J, Forouzanfar MH, et al. Worldwide epidemiology of atrial fibrillation: A Global Burden of Disease 2010 study. Circulation. 2014; 129:837–847. [PubMed: 24345399]
3. Dobrev D, Nattel S. New antiarrhythmic drugs for treatment of atrial fibrillation. Lancet. 2010; 375:1212–1223. [PubMed: 20334907]
4. Al-Khatib SM, Allen LaPointe NM, Chatterjee R, Crowley MJ, Dupre ME, Kong DF, Lopes RD, Povsic TJ, Raju SS, Shah B, Kosinski AS, et al. Rate- and rhythm-control therapies in patients with atrial fibrillation: A systematic review. Ann Intern Med. 2014; 160:760–773. [PubMed: 24887617]
5. Allessie M, Ausma J, Schotten U. Electrical, contractile and structural remodeling during atrial fibrillation. Cardiovasc Res. 2002; 54:230–246. [PubMed: 12062329]
6. Tamargo J, Caballero R, Gómez R, Delpón E. Cardiac electrophysiological effects of nitric oxide. Cardiovasc Res. 2010; 87:593–600. [PubMed: 20587506]
7. Cai H, Li Z, Goette A, Mera F, Honeycutt C, Feterik K, Wilcox JN, Dudley SC Jr, Harrison DG, Langberg JJ. Downregulation of endocardial nitric oxide synthase expression and nitric oxide production in atrial fibrillation: Potential mechanisms for atrial thrombosis and stroke. Circulation. 2002; 106:2854–2858. [PubMed: 12451014]
8. Shiroshita-Takeshita A, Brundel BJJM, Burstein B, Leung T-K, Mitamura H, Ogawa S, Nattel S. Effects of simvastatin on the development of the atrial fibrillation substrate in dogs with congestive heart failure. Cardiovasc Res. 2007; 74:75–84. [PubMed: 17270161]
9. Williams JC, Armesilla AL, Mohamed TMA, Hagarty CL, McIntyre FH, Schomburg S, Zaki AO, Oceandy D, Cartwright EJ, Buch MH, Emerson M, et al. The sarcolemmal calcium pump, α-1 syntrophin, and neuronal nitric-oxide synthase are parts of a macromolecular protein complex. J Biol Chem. 2006; 281:23341–23348. [PubMed: 16735509]

10. Zhang YH, Casadei B. Sub-cellular targeting of constitutive NOS in health and disease. J Mol Cell Cardiol. 2012; 52:341–350. [PubMed: 21945464]
11. Jian Z, Han H, Zhang T, Puglisi J, Izu LT, Shaw JA, Onofiok E, Erickson JR, Chen Y-J, Horvath B, Shimkunas R, et al. Mechanochemotransduction during cardiomyocyte contraction is mediated by localized nitric oxide signaling. Sci Signaling. 2014; 7:ra27.
12. Thomas GD, Sander M, Lau KS, Huang PL, Stull JT, Victor RG. Impaired metabolic modulation of α-adrenergic vasoconstriction in dystrophin-deficient skeletal muscle. Proc Natl Acad Sci USA. 1998; 95:15090–15095. [PubMed: 9844020]
13. Seddon M, Melikian N, Dworakowski R, Shabeeh H, Jiang B, Byrne J, Casadei B, Chowienczyk P, Shah AM. Effects of neuronal nitric oxide synthase on human coronary artery diameter and blood flow in vivo. Circulation. 2009; 119:2656–2662. [PubMed: 19433760]
14. Brenman JE, Chao DS, Xia H, Aldape K, Bredt DS. Nitric oxide synthase complexed with dystrophin and absent from skeletal muscle sarcolemma in Duchenne muscular dystrophy. Cell. 1995; 82:743–752. [PubMed: 7545544]
15. Sander M, Chavoshan B, Harris SA, Iannaccone ST, Stull JT, Thomas GD, Victor RG. Functional muscle ischemia in neuronal nitric oxide synthase-deficient skeletal muscle of children with Duchenne muscular dystrophy. Proc Natl Acad Sci USA. 2000; 97:13818–13823. [PubMed: 11087833]
16. Cacchiarelli D, Incitti T, Martone J, Cesana M, Cazzella V, Santini T, Sthandier O, Bozzoni I. miR-31 modulates dystrophin expression: New implications for Duchenne muscular dystrophy therapy. EMBO Rep. 2011; 12:136–141. [PubMed: 21212803]
17. Britton OJ, Bueno-Orovio A, Van Ammel K, Lu HR, Towart R, Gallacher DJ, Rodriguez B. Experimentally calibrated population of models predicts and explains intersubject variability in cardiac cellular electrophysiology. Proc Natl Acad Sci USA. 2013; 110:E2098–E2105. [PubMed: 23690584]
18. Chang WJ, Iannaccone ST, Lau KS, Masters BS, McCabe TJ, McMillan K, Padre RC, Spencer MJ, Tidball JG, Stull JT. Neuronal nitric oxide synthase and dystrophin-deficient muscular dystrophy. Proc Natl Acad Sci USA. 1996; 93:9142–9147. [PubMed: 8799168]
19. Voigt N, Heijman J, Wang Q, Chiang DY, Li N, Karck M, Wehrens XH, Nattel S, Dobrev D. Cellular and molecular mechanisms of atrial arrhythmogenesis in patients with paroxysmal atrial fibrillation. Circulation. 2014; 129:145–156. [PubMed: 24249718]
20. Workman AJ, Pau D, Redpath CJ, Marshall GE, Russell JA, Kane KA, Norrie J, Rankin AC. Post-operative atrial fibrillation is influenced by beta-blocker therapy but not by pre-operative atrial cellular electrophysiology. J Cardiovasc Electrophysiol. 2006; 17:1230–1238. [PubMed: 17074009]
21. Hutvagner G, Simard MJ. Argonaute proteins: Key players in RNA silencing. Nat Rev Mol Cell Biol. 2008; 9:22–32. [PubMed: 18073770]
22. Luo X, Yang B, Nattel S. MicroRNAs and atrial fibrillation: Mechanisms and translational potential. Nat Rev Cardiol. 2015; 12:80–90. [PubMed: 25421165]
23. Cacchiarelli D, Martone J, Girardi E, Cesana M, Incitti T, Morlando M, Nicoletti C, Santini T, Sthandier O, Barberi L, Auricchio A, et al. MicroRNAs involved in molecular circuitries relevant for the Duchenne muscular dystrophy pathogenesis are controlled by the dystrophin/nNOS pathway. Cell Metab. 2010; 12:341–351. [PubMed: 20727829]
24. Shirokova N, Niggli E. Cardiac phenotype of Duchenne Muscular Dystrophy: Insights from cellular studies. J Mol Cell Cardiol. 2013; 58:217–224. [PubMed: 23261966]
25. Reilly SN, Jayaram R, Nahar K, Antoniades C, Verheule S, Channon KM, Alp NJ, Schotten U, Casadei B. Atrial sources of reactive oxygen species vary with the duration and substrate of atrial fibrillation: Implications for the antiarrhythmic effect of statins. Circulation. 2011; 124:1107–1117. [PubMed: 21844076]
26. Idigo WO, Reilly S, Zhang MH, Zhang YH, Jayaram R, Carnicer R, Crabtree MJ, Balligand J-L, Casadei B. Regulation of endothelial nitric-oxide synthase (NOS) *S*-glutathionylation by neuronal NOS: Evidence of a functional interaction between myocardial constitutive NOS isoforms. J Biol Chem. 2012; 287:43665–43673. [PubMed: 23091050]

27. Gómez R, Núñez L, Vaquero M, Amorós I, Barana A, de Prada T, Macaya C, Maroto L, Rodriguez E, Caballero R, López-Farré A, et al. Nitric oxide inhibits Kv4.3 and human cardiac transient outward potassium current (I_{to1}). Cardiovasc Res. 2008; 80:375–384. [PubMed: 18678642]

28. Gómez R, Caballero R, Barana A, Amorós I, Calvo E, López JA, Klein H, Vaquero M, Osuna L, Atienza F, Almendral J, et al. Nitric oxide increases cardiac IK1 by nitrosylation of cysteine 76 of Kir2.1 channels. Circ Res. 2009; 105:383–392. [PubMed: 19608980]

29. Schotten U, Verheule S, Kirchhof P, Goette A. Pathophysiological mechanisms of atrial fibrillation: A translational appraisal. Physiol Rev. 2011; 91:265–325. [PubMed: 21248168]

30. Cappato R, Calkins H, Chen S-A, Davies W, Iesaka Y, Kalman J, Kim Y-H, Klein G, Packer D, Skanes A. Worldwide survey on the methods, efficacy, and safety of catheter ablation for human atrial fibrillation. Circulation. 2005; 111:1100–1105. [PubMed: 15723973]

31. van Rooij E, Purcell AL, Levin AA. Developing microRNA therapeutics. Circ Res. 2012; 110:496–507. [PubMed: 22302756]

32. Schotten U, Duytschaever M, Ausma J, Eijsbouts S, Neuberger H-R, Allessie M. Electrical and contractile remodeling during the first days of atrial fibrillation go hand in hand. Circulation. 2003; 107:1433–1439. [PubMed: 12642366]

33. Cox B, Emili A. Tissue subcellular fractionation and protein extraction for use in mass-spectrometry-based proteomics. Nat Protoc. 2006; 1:1872–1878. [PubMed: 17487171]

34. Verheule S, Sato T, Everett TT IV, Engle SK, Otten D, Rubart-von der Lohe M, Nakajima HO, Nakajima H, Field LJ, Olgin JE. Increased vulnerability to atrial fibrillation in transgenic mice with selective atrial fibrosis caused by overexpression of TGF-β1. Circ Res. 2004; 94:1458–1465. [PubMed: 15117823]

35. Maleckar MM, Greenstein JL, Giles WR, Trayanova NA. K^+ current changes account for the rate dependence of the action potential in the human atrial myocyte. Am J Physiol Heart Circ Physiol. 2009; 297:H1398–H1410. [PubMed: 19633207]

Europe PMC Funders Author Manuscripts

Europe PMC Funders Author Manuscripts

Editor's Summary

Rhythm remodeling traced to tiny RNA

Atrial fibrillation (AF) is characterized by abnormal heart rhythms and can be caused by a variety of risk factors ranging from obesity to diabetes. Although treatments exist, AF is famously able to recur by "remodeling" the heart tissue electrically and structurally to maintain its unsteady beat. Reilly *et al.* have discovered a small noncoding RNA, miR-31, that is responsible for a string of signals that allowfor such remodeling. An increase in miR-31 led to depletion of neuronal nitric oxide synthase (nNOS) and repression of dystrophin (which binds nNOS in muscle cells) in the fibrillating atrial myocardium of both humans and goats. These mechanistic findings were further explored in mice. Because up-regulation of miR-31 and the resulting loss of dystrophin and nNOS in AF are specific to the atrium, it may be possible to target interventions to this remodeling pathway, thus providing a safer therapeutic option for patients with AF than those that are currently available, including ablation and ion channel blockers.

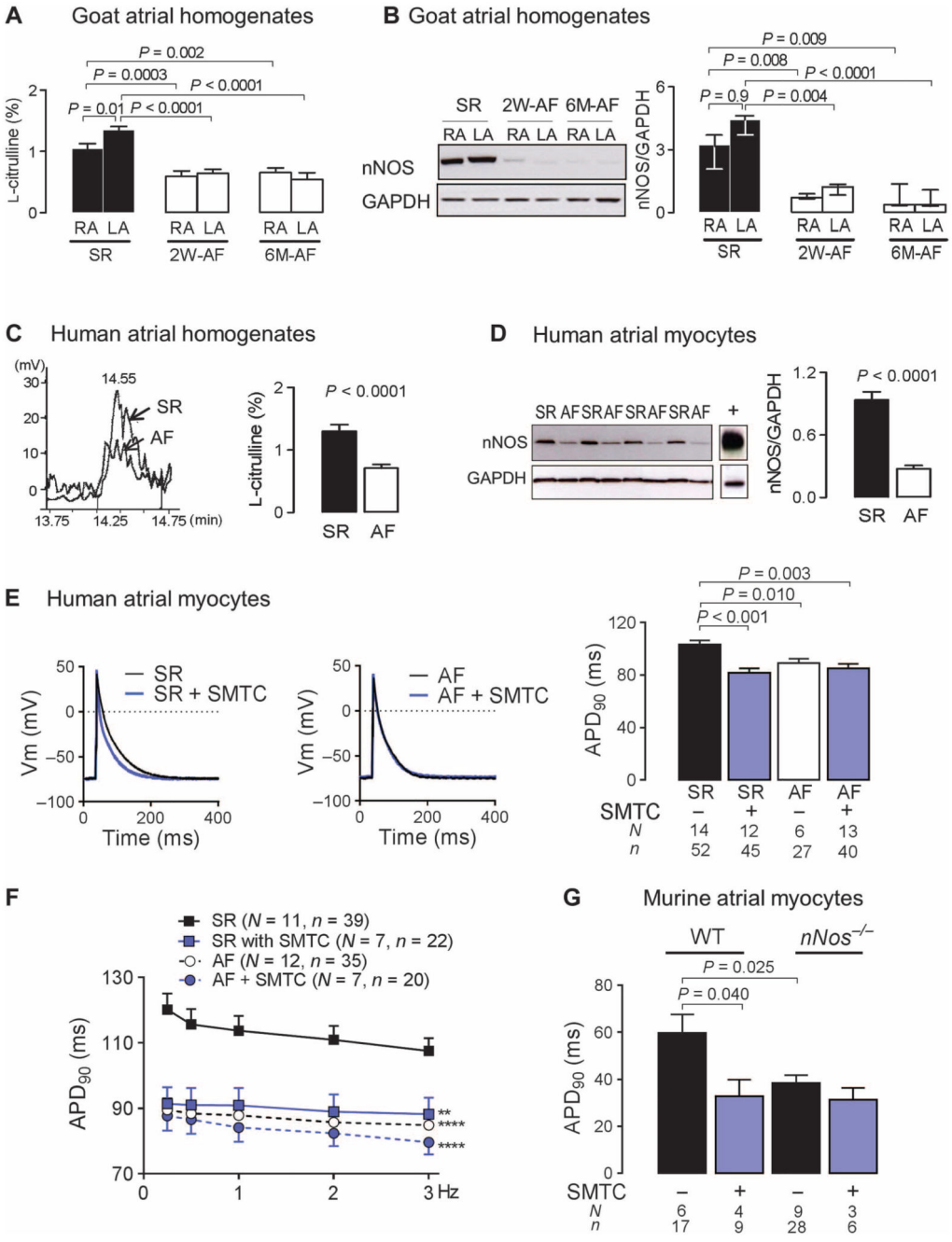

Fig. 1. Loss of atrial nNOS in AF contributes to atrial electrical remodeling.

(**A**) Atrial NOS activity (percent conversion of L-arginine to L-citrulline, reflecting NO synthesis) in right atrial (RA) and left atrial (LA) tissues from goats at 2 weeks (2W) or 6 months (6M) of AF (n = 6 to 8) or SR (n = 9 to 11). Data are averages ± SEM. P values were determined by one-way analysis of variance (ANOVA) with Bonferroni correction. (**B**) nNOS immunoblots in goat atrial tissue at 2 weeks or 6 months of AF (n = 6 to 8) or SR (n = 9 to 11). Data are medians and interquartile ranges. P values were determined by Kruskal-Wallis test. GAPDH, glyceraldehyde-3-phosphate dehydrogenase. (**C**) Representative

chromatograms of L-citrulline production (left) and average atrial NOS activity ± SEM (right) in RA samples from patients in SR (n = 17) or AF (n = 19). P value was determined by unpaired t test. (**D**) nNOS protein content in human RA myocytes from patients in SR (n = 19) or AF (n = 12). Murine brain was used as positive control for nNOS (lane marked with +). Data are averages ± SEM. P value was determined by unpaired t test. (**E**) Effect of nNOS inhibition with SMTC on APD_{90} in RA myocytes from patients in SR or AF. Representative action potential traces (left panel) and average APD_{90} ± SEM (right panel). P values were determined by one-way ANOVA with Bonferroni correction. Vm, membrane potential. (**F**) Frequency-dependent change in APD_{90} in RA myocytes from patients in SR or AF in the presence or absence of SMTC. Data are averages ± SEM. $^{**}P < 0.01$, $^{****}P < 0.0001$ versus SR; $P = 0.0003$ for the interaction between groups and stimulation frequency (not shown), by two-way ANOVA with Bonferroni correction. (**G**) The effect of nNOS inhibition or gene deletion on APD_{90} in murine RA myocytes. Data are averages ± SEM. P values were determined by one-way ANOVA with Bonferroni correction. In (E) to (G), N is the number of animals, whereas n is the number of cells. WT, wild type.

Europe PMC Funders Author Manuscripts

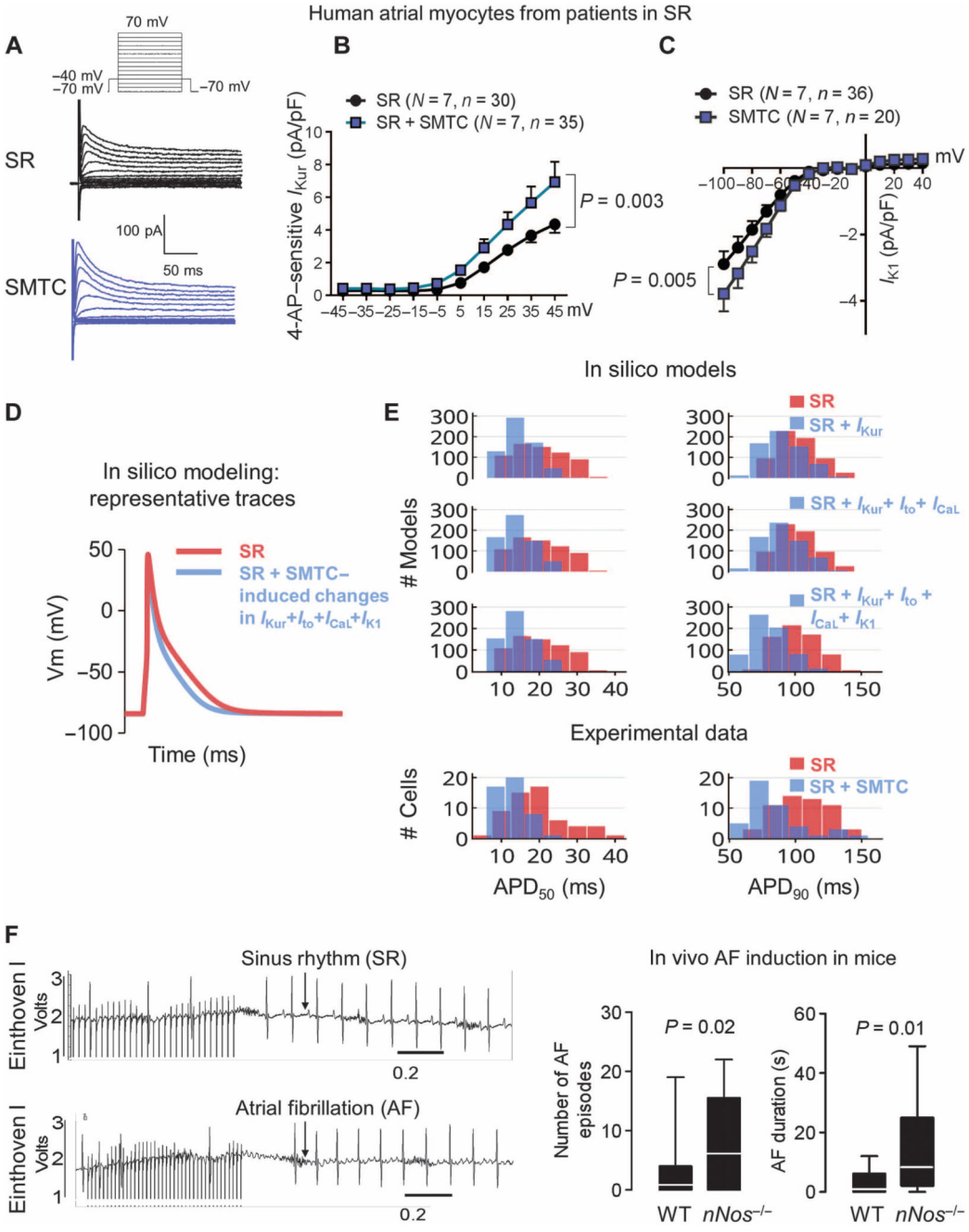

Fig. 2. nNOS disruption increases potassium currents and promotes AF induction in mice.

(**A**) Representative traces of the transient outward K^+ current, elicited by the voltage protocol above, in atrial myocytes from patients in SR in the presence or absence of nNOS inhibition with SMTC. (**B** and **C**) Average current-voltage relationship of the 4-aminopyridine (4-AP)–sensitive ultrarapid delayed rectifier current, I_{Kur} (B), and the inward rectifier current, I_{K1} (C), in the presence or absence of SMTC. Data are averages ± SEM. *N*, number of patients; *n*, number of cells. *P* values for the interaction between voltage and treatment (SMTC) were determined by two-way repeated-measures ANOVA with

Bonferroni correction. (**D**) Simulation of the effect of the changes in ion current density elicited by SMTC on the atrial action potential in an in silico population of human atrial SR models ($n = 640$). (**E**) In silico evaluation of the impact of the increases in ion current density elicited experimentally by nNOS inhibition on the APD_{50} and APD_{90} of human atrial myocytes. Experimental data in atrial myocytes are shown below for comparison. (**F**) Probability of AF induction by atrial burst pacing and duration of the induced AF episodes in WT ($n = 19$) and *nNos*$^{-/-}$ mice ($n = 18$) in vivo. Representative electrocardiogram (ECG) traces after atrial burst pacing (left) and median values with 95% confidence intervals (right). *P* values were determined by Mann-Whitney *U* test.

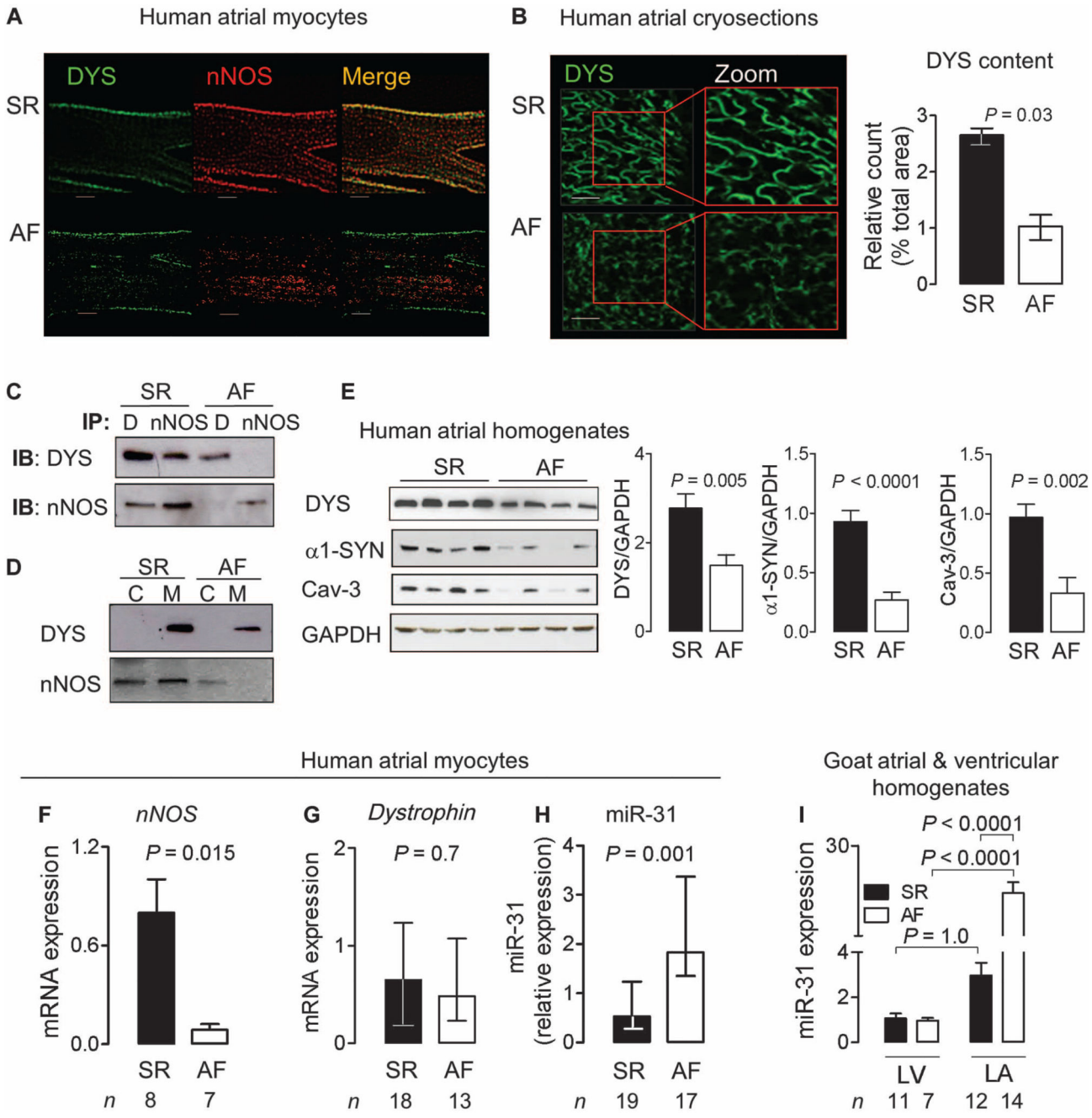

Fig. 3. Loss of dystrophin and miR-31 up-regulation in human AF.

(**A** and **B**) Immunostaining for nNOS and dystrophin (DYS) in atrial myocytes or cryosections from patients in SR or AF. Scale bars, 20 μm. Data in the bar graph are medians with interquartile ranges ($n = 4$ per group). P value was determined by Mann-Whitney U test. (**C**) Dystrophin (DYS or D) and nNOS immunoprecipitation (IP) and immunoblotting (IB) ($n = 5$ biological repeats per group). (**D**) Immunoblots of dystrophin and nNOS in the membrane (M) and cytosolic (C) fraction of atrial tissue homogenates from patients in SR or AF ($n = 4$ biological repeats per group). (**E**) Immunoblots for dystrophin, α1-syntrophin

(α1-SYN), and caveolin-3 (Cav-3) in atrial tissue from patients in SR (n = 9) or AF (n = 10). Data are averages ± SEM. P values were determined by unpaired t test. (**F**) *nNOS* mRNA expression in atrial myocytes from patients in SR or AF. (**G**) *Dystrophin* mRNA expression in atrial myocytes from patients in SR or AF. (**H**) miR-31 expression in atrial myocytes from patients in SR or AF. Transcripts were normalized to *GAPDH* (*dystrophin* and *nNOS*) or *snoU6* (miR-31). Data are averages ± SEM (F) or medians and interquartile ranges (G and H). P values were determined by unpaired t test (F) or Mann-Whitney U test (G and H). (**I**) miR-31 expression in left ventricular (LV) and left atrial (LA) tissue from goats in SR (n = 11) or AF (n = 7). Data are averages ± SEM. P values were determined by one-way ANOVA with Bonferroni correction.

Europe PMC Funders Author Manuscripts

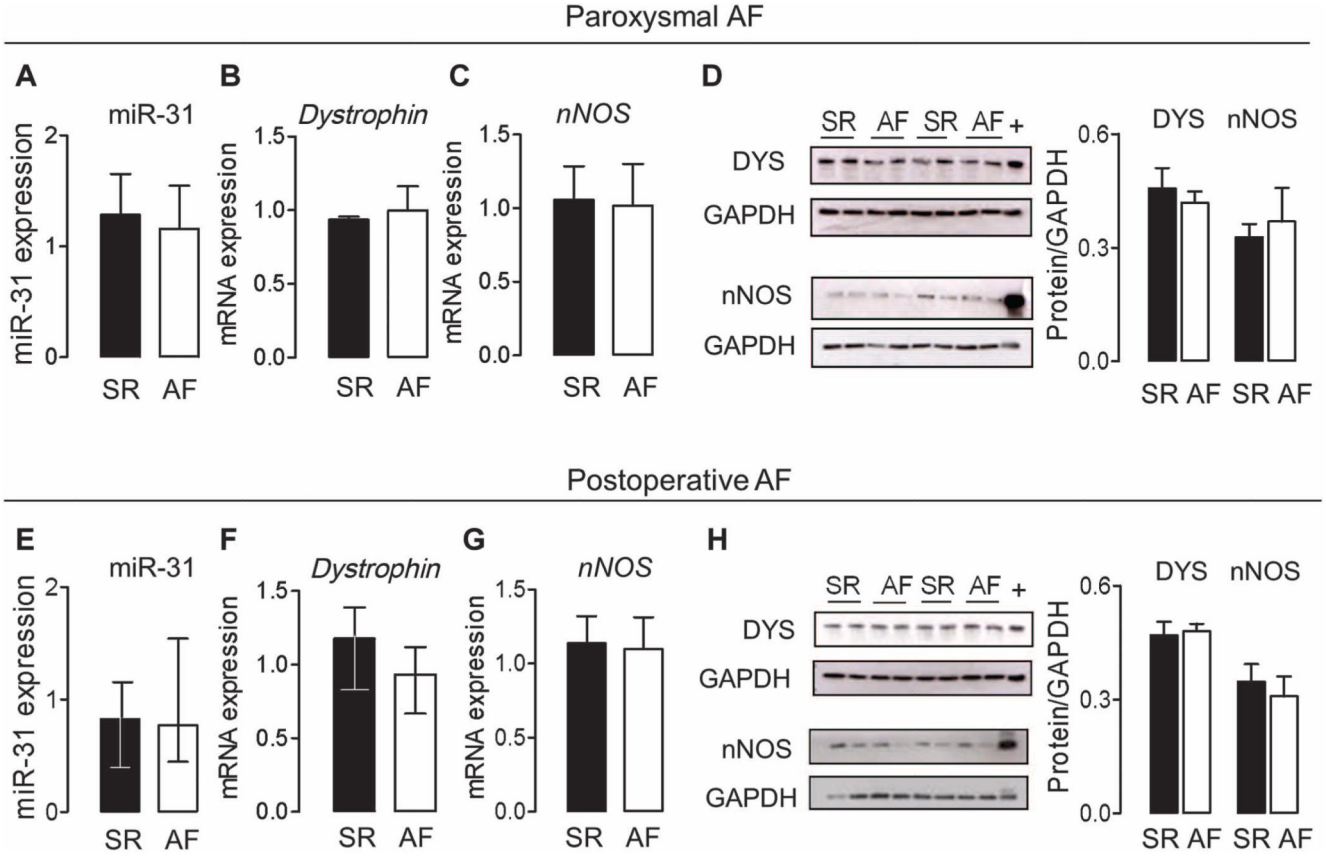

Fig. 4. Atrial miR-31, dystrophin, and nNOS in patients with paroxysmal AF and in those who developed AF after cardiac surgery.

(**A** to **D**) Expression of miR-31 (A), *dystrophin* (B), and *nNOS* (C) mRNA and dystrophin and nNOS immunoblots (D) in right atrial tissue from patients with paroxysmal AF (n = 5 to 8) or SR (n = 6 to 8). The positive control for nNOS and dystrophin (indicated by +) is murine skeletal muscle. Data are averages ± SEM. (**E** to **H**) Expression of miR-31 (E), *dystrophin* (F) and *nNOS* (G) mRNA and dystrophin and nNOS immunoblots (H) in right atrial tissue from patients in SR who developed AF after cardiac surgery (n = 18 to 12) versus those who remained in SR postoperatively (n = 8 to 11). The positive control for nNOS and dystrophin (indicated by +) is murine skeletal muscle. Data are medians and interquartile ranges (E and F) or averages ± SEM (G and H). All comparisons (A to H) between SR and AF were not significant [unpaired t test or Mann-Whitney U test (E and F)].

Europe PMC Funders Author Manuscripts

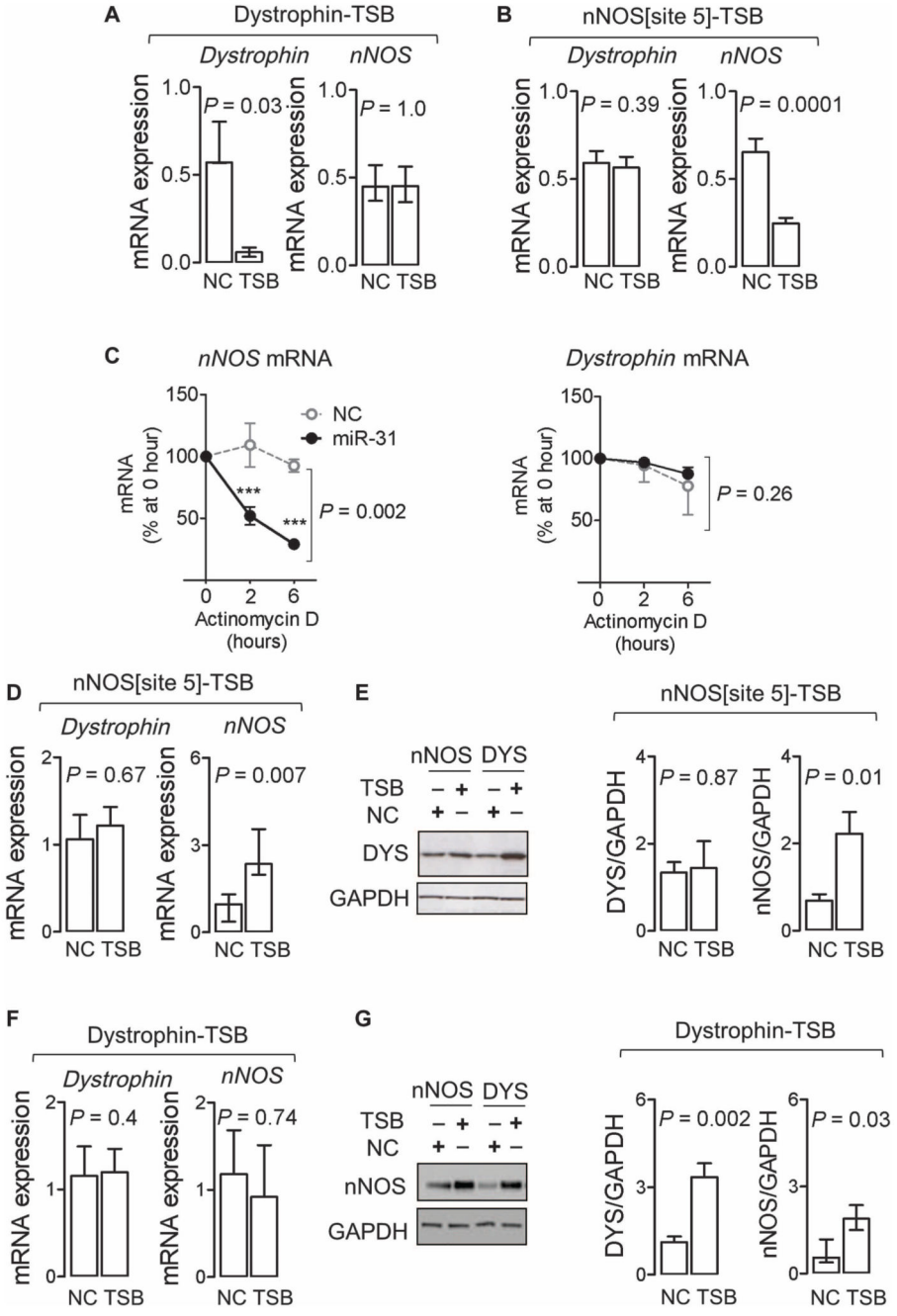

Fig. 5. miR-31 targets *dystrophin* and *nNOS* mRNA.

(**A**) Effect of an miR-3' TSB on the *dystrophin* 3′UTR ($n = 9$) [versus non-targeting control (NC); $n = 7$] on *dystrophin* and *nNOS* transcripts in Ago2 immunoprecipitates in atrial myocytes from patients with AF. Data are medians and interquartile ranges. *P* values were determined by Wilcoxon matched pairs test. (**B**) Effect of an miR-31 TSB for site 5 on the *nNOS* 3'UTR ($n = 9$) versus NC ($n = 7$) on *dystrophin* and *nNOS* transcripts in Ago2 immunoprecipitates in atrial myocytes from patients with AF. Transcripts were normalized to miR-31. Data are averages ± SEM. *P* values were determined by paired *t* test. (**C**) Effect

of an miR-31 mimic (n=4 to 7) or NC (n = 4 per group) on the rate of decay of *nNOS* and *dystrophin* mRNA (normalized to *GAPDH*) in actinomycin D–treated atrial myocytes from patients in SR (expressed as percentage of the respective mRNA at 0 hour). Data are averages ± SD. ***P < 0.001 versus NC at the respective time point; P value is also given for the interaction between treatments (NC and miR-31 mimic) and time, by two-way ANOVA with Bonferroni correction. (**D** and **E**) Effect of *nNOS*[site5]-TSB (n = 8) or NC (n = 5) on *nNOS* or *dystrophin* mRNA (D) and protein content (E) in atrial myocytes from patients with AF. Data are averages ± SEM except for *nNOS* in (D), which are medians and interquartile ranges. P values were determined by unpaired t test or Mann-Whitney U test [for *nNOS* in (D)]. (**F** and **G**) Effect of dystrophin-TSB (n = 5) or NC (n = 5) on *nNOS* or *dystrophin* mRNA (F) and protein content (G) in atrial myocytes from patients with AF. Data are averages ± SEM except for nNOS in (G), which are medians and interquartile ranges. P values were determined by unpaired t test or Mann-Whitney U test [for nNOS in (G)].

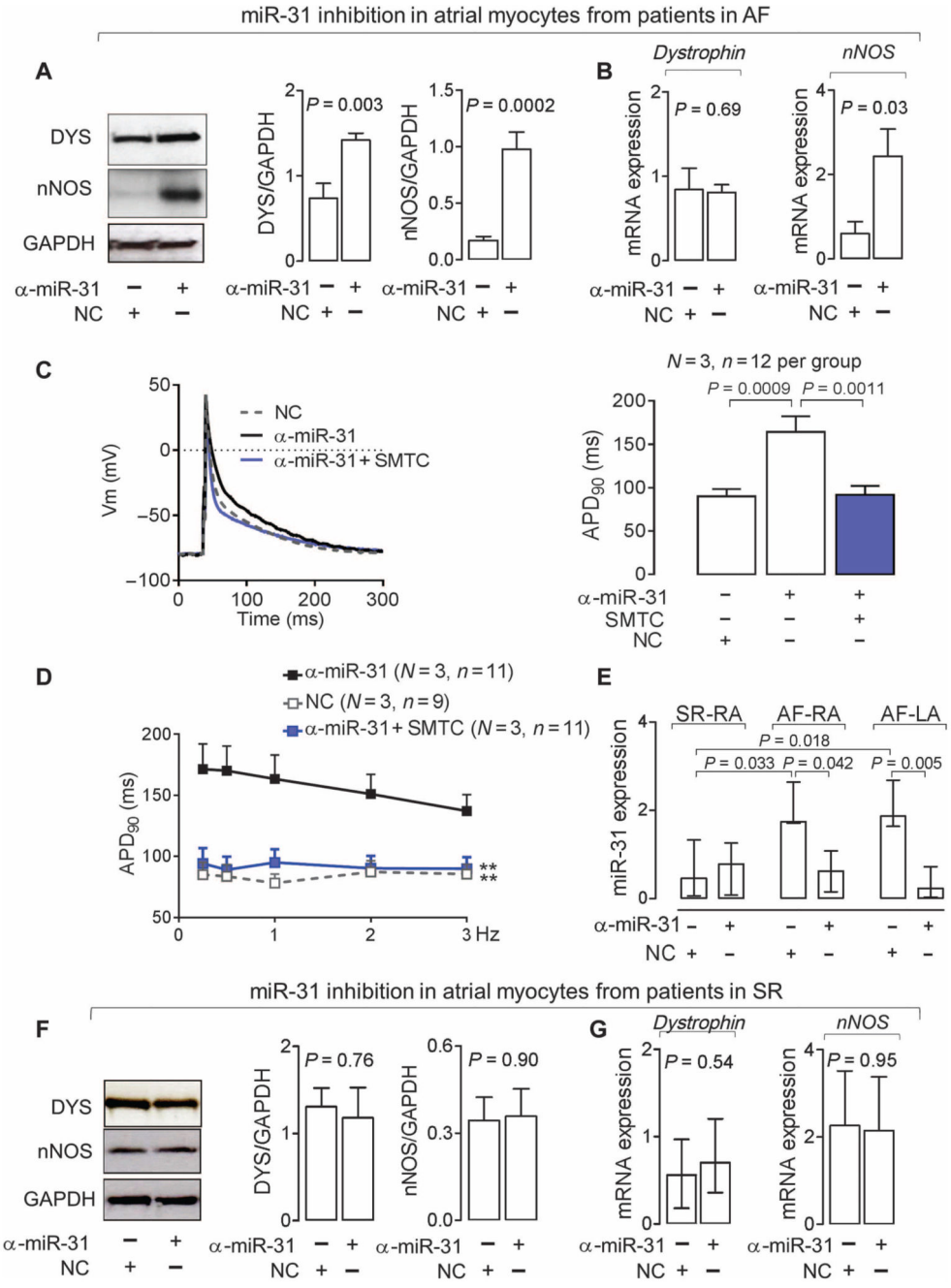

Fig. 6. Inhibition of miR-31 recovers nNOS and dystrophin and restores APD in AF.

(**A** and **B**) Effect of an miR-31 inhibitor (α-miR-31; $n = 9$) or a nontargeting negative control (NC; $n = 5$ to 9) on nNOS or dystrophin protein and mRNA in atrial myocytes from patients with AF. Data are averages ± SEM. P values were determined by paired t test (A) or unpaired t test (B) when the tissue sample was not sufficient to provide aliquots for paired comparisons of miR-31 inhibition and NC. (**C**) APD_{90} of atrial myocytes from patients with AF treated with α-miR-31 in the presence or absence of the nNOS inhibitor SMTC. Left: representative data traces. Right: Averages ± SEM. P values were determined by one-way

ANOVA with Bonferroni correction. (**D**) APD_{90} rate-dependent adaptation in atrial myocytes from patients with AF treated with α-miR-31 in the presence or absence of SMTC. Data are averages ± SEM. $^{**}P < 0.01$ versus α-miR-31; $P < 0.0001$ for the interaction between treatment and frequency (not shown), by two-way repeated-measures ANOVA with Bonferroni correction. (**E**) Effect of α-miR-31 or NC on miR-31 expression in atrial myocytes from patients with AF ($n = 4$ to 6) or SR ($n = 5$ to 6). Data are medians and interquartile ranges. *P* values were determined by Kruskal-Wallis with Dunn's correction. (**F** and **G**) Effect of α-miR-31 or NC on protein (F) or mRNA expression (G) of dystrophin (protein, $n = 7$ per group; mRNA, $n = 6$ per group) or nNOS (protein, $n = 5$ to 6; mRNA, $n = 4$ to 5 per group) in atrial myocytes from patients in SR. Data are averages ± SEM except for *dystrophin* in (G), which are medians and interquartile ranges. *P* values were determined by unpaired *t* test or Mann-Whitney *U* test [for *dystrophin* in (G)].

Europe PMC Funders Author Manuscripts

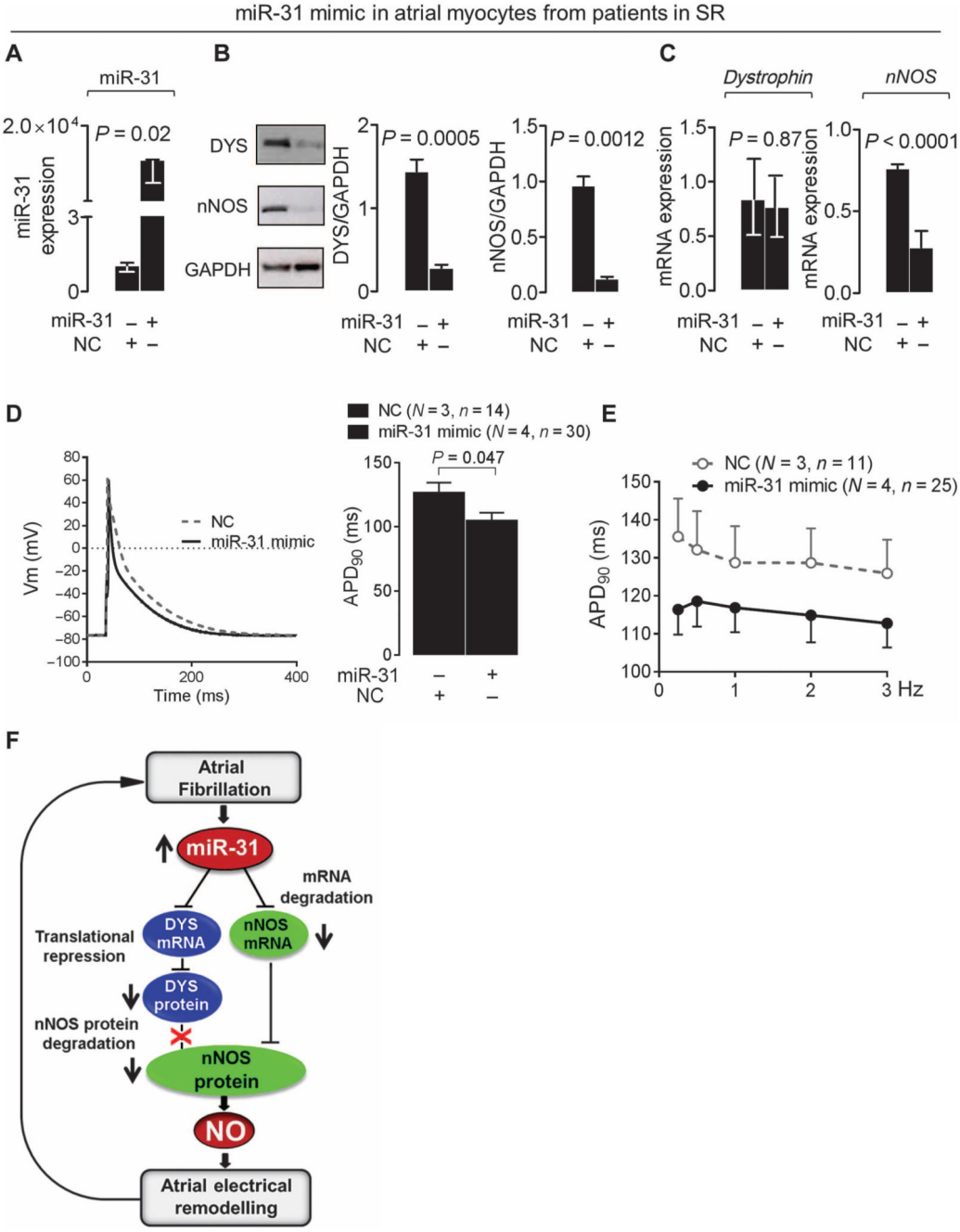

Fig. 7. miR-31 overexpression depletes nNOS and dystrophin and shortens APD in SR.

(**A** to **C**) Effect of miR-31 overexpression with an miR-31 mimic [versus nontargeting control (NC) (A)] on dystrophin and nNOS protein [$n = 5$ per group (B)] or mRNA [$n = 5$ to 9 (C)] in atrial myocytes from patients in SR. Data are averages ± SEM except for miR-31 (A) and dystrophin (C), where they are medians and interquartile ranges. *P* values were determined by unpaired *t* test or Mann-Whitney *U* test [miR-31 in (A) and dystrophin in (C)]. (**D**) APD_{90} in SR atrial myocytes treated with an miR-31 mimic or NC. Left: Representative data traces. Right: Average values ± SEM. *P* value was determined by

unpaired *t* test. (**E**) APD_{90} rate-dependent adaptation in SR myocytes treated with an miR-31 mimic or NC. Data are averages ± SEM. $P = 0.227$ for the effect of treatment with the miR-31 mimic, and $P = 0.378$ for the interaction between treatment and frequency by two-way repeated-measures ANOVA. In (D) and (E), *N* is the number of patients, and *n* is the number of cells. (**F**) Summary diagram of the main findings: atrial miR-31 up-regulation in atrial myocytes from patients with AF accelerates *nNOS* mRNA decay and alters nNOS subcellular localization and protein stability by inhibiting *dystrophin* translation. The resulting reduction in nNOS-derived NO contributes to the AF-induced electrical remodeling and, thus, to the maintenance and progression of AF.

Europe PMC Funders Author Manuscripts